

# DreamLoop: Controllable Cinemagraph Generation from a Single Photograph

Aniruddha Mahapatra Long Mai Cusuh Ham Feng Liu

Adobe Research

<https://anime26398.github.io/dreamloop.github.io/>

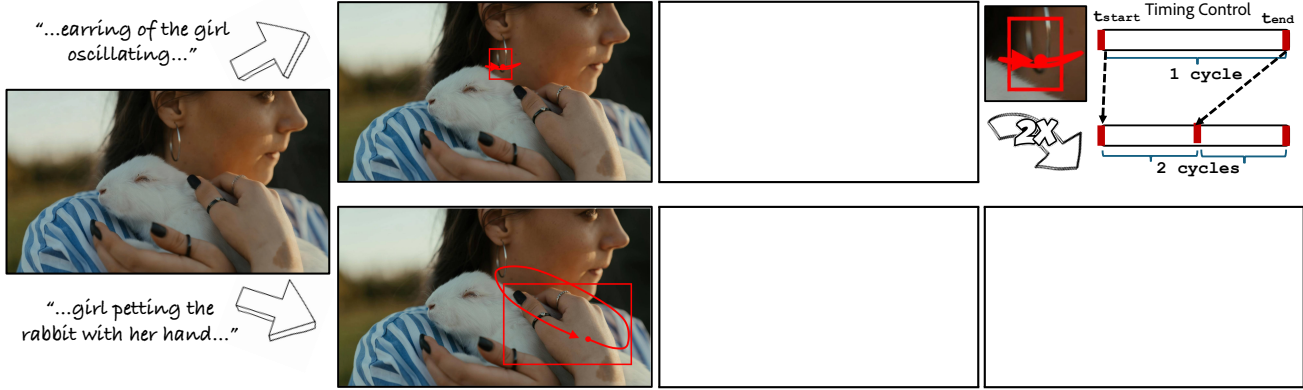


Figure 1. **Teaser.** Starting with the same input photograph, we showcase *DreamLoop*’s capability to let user generate diverse cinemagraphs with precise motion control. (top-middle) the user intends to animate the earring of the girl, oscillating. (bottom-middle) the user simulates the action of ‘girl petting the rabbit’. *DreamLoop*’s generates high-quality cinemagraph following user input in both cases. User can also play with timing control, (left) user doubles the oscillating frequency of the girls earring and *DreamLoop* accurately captures it. *We encourage readers to view the videos in the figure with Acrobat Reader.*

## Abstract

Cinemagraphs, which combine static photographs with selective, looping motion, offer unique artistic appeal. Generating them from a single photograph in a controllable manner is particularly challenging. Existing image-animation techniques are restricted to simple, low-frequency motions and operate only in narrow domains with repetitive textures like water and smoke. In contrast, large-scale video diffusion models are not tailored for cinemagraph constraints and lack the specialized data required to generate seamless, controlled loops. We present **DreamLoop**, a controllable video synthesis framework dedicated to generating cinemagraphs from a single photo without requiring any cinemagraph training data. Our key idea is to adapt a general video diffusion model by training it on two objectives: temporal bridging and motion conditioning. This strategy enables flexible cinemagraph generation. During inference, by using the input image as both the first- and last- frame condition, we enforce a seamless loop. By conditioning on static tracks, we maintain a static background. Finally, by providing a

user-specified motion path for a target object, our method provides intuitive control over the animation’s trajectory and timing. To our knowledge, *DreamLoop* is the first method to enable cinemagraph generation for general scenes with flexible and intuitive controls. We demonstrate that our method produces high-quality, complex cinemagraphs that align with user intent, outperforming existing approaches.

## 1. Introduction

Cinemagraph is an art form that combines the appeal of static images and dynamic videos. It depicts a scene where most elements are static, while a few selected regions move in a seamless, looping manner. While this medium is popular in creative communities, its creation remains a significant challenge. The conventional process demands a carefully planned video shoot, tripod stabilization, and tedious post-production for motion segmentation and frame blending. Generating a cinemagraph from a single photograph offers a promising way to make this art form more accessible.

However, this task presents a unique set of challenges distinct from standard image-to-video (I2V) generation. First, the animation must be selective; unlike typical I2V models [26, 51, 60] that animate all plausible elements, a cinemagraph requires keeping most of the scene static to preserve its photographic nature. Second, the generated motion must be seamlessly looping to be played infinitely. Finally, the process must be highly controllable, allowing users to define which regions move, how they move (e.g., path, direction), and the timing of that motion (e.g., speed, looping frequency).

Existing single-image-to-cinemagraph methods [14, 18, 22, 38, 47] are limited to narrow domains with repetitive textures (‘*fluid elements*’ [37]) and can animate only simple motions such as water, smoke, etc. A major limitation of these approaches is that most of them [14, 18, 22, 37, 38] rely predominantly on optical flow prediction, resulting in *in-place* motion of repeating textures; thus, they are fundamentally incapable of animating general scene elements, such as humans, animals, or everyday objects, as shown in Figure 1. On the other hand, large-scale video diffusion models, while powerful, are not designed for these specific constraints. They struggle to maintain a static background, do not inherently produce loops, and lack the fine-grained motion control necessary for artistic cinemagraph creation. Furthermore, training a dedicated model is hampered by the lack of large-scale, high-quality cinemagraph datasets.

In this paper, we present a novel framework for generating high-quality, controllable cinemagraph from a single image, without requiring cinemagraph data for training. Our central idea is to adapt a standard video diffusion model (VDM) trained on general video data to this specific task. We achieve this by augmenting the VDM with two key conditioning signals during training: (1) a video bridging objective, where the model learns to generate intermediate frames given the first and last frames, and (2) a motion anchoring objective, where the model learns to generate video conditioned on explicit motion signals, including bounding box sequence and sparse point tracks.

This training strategy enables flexible and fully controllable cinemagraph generation. At inference time, to achieve a seamless loop, we use the input photograph as both the first and last frames, forcing the model to generate a perfectly looping sequence. To ensure a static background, we provide static motion tracks for background regions. Finally, user control is achieved by allowing the user to specify a motion path for a selected object, which serves as the motion-conditioning signal. This allows for intuitive control over the motion trajectory and timing from a single input image. To the best of our knowledge, this is the first method to enable cinemagraph generation from a single image of a general scene with such flexible and intuitive control. We demonstrate that our method can produce high-quality, complex

cinemagraphs that align with user intent, outperforming existing approaches. Despite being trained on general videos, our method even surpasses specialized cinemagraph methods on fluid-element domains such as water and smoke.

In summary, this paper makes the following contributions:

- We introduce the first method capable of generating cinemagraphs from general-purpose photographs—not limited to fluid elements—by finetuning a pretrained image-to-video diffusion model with (1) first–last frame conditioning for seamless looping and (2) motion conditioning via bounding-box sequences and sparse point tracks for precise motion control.
- We propose a user-friendly and intuitive control framework (and accompanying UI) that enables users to specify object trajectories, motion paths, and background constraints, enabling precise and flexible cinemagraph creation from a single input image.

## 2. Related Work

**Video Looping and Cinemagraph.** Classic cinemagraph creation methods typically operate on real videos containing periodic motion. The seminal Video Textures approach [45] introduced a graph-based formulation to identify visually consistent frame transitions, enabling seamless looping. Subsequent works [3, 25, 27, 49] extend this idea by decomposing a scene into dynamic and static regions, often requiring user-provided masks or careful video stabilization to isolate looping elements. Other methods [32, 33] allow different regions to loop at independent paces, while additional efforts explore handling challenging settings such as moving cameras [46], portraits [4], and panoramic imagery [1, 20]. A key limitation of these video-based methods is that they require an input video captured with a very stable camera setup, which typically demands substantial effort, user guidance, and equipment such as tripods or controlled environments. In contrast, our method enables cinemagraph creation directly from a single photograph, greatly reducing the required user effort while still generating highly controllable animation.

**Single Image Animation.** Another line of work generates cinemagraphs by starting from a single image and synthesizing periodic motion. One of the earliest efforts is by Chuang *et al.* who manually specify motion priors for different semantic categories such as water and leaves [12]. More recent approaches leverage deep networks to predict motion fields [6, 14, 15, 18, 22, 30, 35, 37]. Animating Landscape predicts motion autoregressively and synthesizes videos via backward warping [14]. Holynski *et al.* instead estimate a single optical-flow field describing motion between consecutive frames and use forward warping to reduce stretching artifacts [22]. Mahapatra *et al.* [37] and Fan *et al.* [15] introduce control mechanisms using user-provided masks and directional cues. A fundamental limitation of these approaches is that they rely heavily on optical-flow prediction,

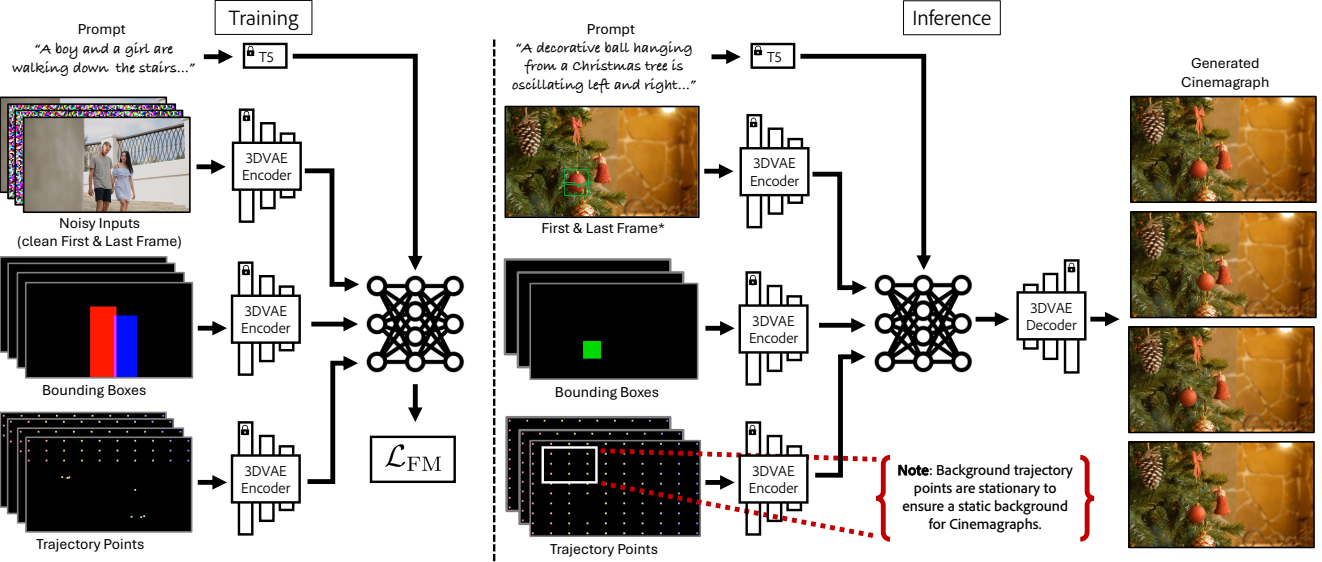


Figure 2. **Methodology.** Figure shows details of our method *DreamLoop*. (left) shows the training procedure with bounding box and sparse point track control. (right) shows the inference setting for generating controllable cinemagraphs with our method.

typically in the form of a single flow map [15, 18, 22, 37, 38]. As a result, they can only animate scenes with repetitive, in-place motions such as water, smoke, or foliage. These methods cannot model the complex non-repetitive dynamics characteristic of rigid objects, including humans, animals, or everyday objects—for example, “*a person applying makeup*” or “*a photographer adjusting a camera lens*” (Figure 5). In contrast, our method is the first to generate cinemagraphs from a single image that works reliably on *general scenes and general motion*, without being limited to fluid elements. **Image-to-Video Generation.** Recent progress in video foundation models [5, 8–10, 17, 43, 57, 60] has enabled highly realistic video generation from a single image and a text prompt. While these models excel at producing diverse and visually compelling videos, their control mechanisms remain largely text-driven. As a result, they cannot provide the fine-grained, spatially localized control over object motion—such as precise trajectories, directional paths, or temporal timing—that cinemagraph creation requires. Moreover, these models are not designed to preserve a static background, nor do they inherently produce seamlessly looping videos, both of which are essential properties of cinemagraphs. In contrast, our method leverages a pretrained image-to-video diffusion model and finetunes it with first–last frame conditioning and explicit motion signals (bounding-box sequences and sparse point tracks).

**Controllable Video Generation.** Recent progress in controllable video synthesis provides a variety of mechanisms for user-guided motion specification. Existing work typically supports one of three major forms of control: (1) Bounding-box control [23, 29, 36, 52, 55], (2) Point-trajectory con-

trol [39, 40, 54, 56], (3) Camera control [2, 19, 53, 54, 61]. More recently, MotionCanvas [58] enables joint control of both camera and object motion. Instead of relying on explicit camera labels—which are expensive and difficult to obtain—they train the model using sparse point trajectories and interpret such motion during inference as camera movement. We draw inspiration from these controllable video-generation approaches and examine the problem of cinemagraph generation through the lens of controllable video synthesis, incorporating additional constraints specific to cinemagraphs.

### 3. Method

Given a user photograph  $I \in \mathbb{R}^{H' \times W' \times 3}$ , a text prompt  $c$ , and motion conditions consisting of  $N$  bounding boxes  $(x_1, y_1, x_2, y_2)_n \in \mathbb{R}^4$  and  $M$  point tracks  $(x, y)_m \in \mathbb{R}^2$  specified for  $T'$  frames, our goal is to synthesize a cinemagraph  $V \in \mathbb{R}^{T' \times H' \times W' \times 3}$  of length  $T'$ . As discussed in Section 1 and 2, most single-image-to-cinemagraph methods rely on predicting optical flow and use a single optical-flow field [15, 18, 22, 37, 38] to animate the input image. This stationary-flow assumption restricts them to scenes with repetitive, in-place motions (e.g., water, smoke) and makes them unsuitable for complex, non-repetitive dynamics of general scene elements such as humans and animals. Our approach targets this general setting by leveraging the strong motion priors of large-scale video diffusion models (VDMs) trained on millions of open-domain videos. We first outline why off-the-shelf VDMs are not directly suitable for cinemagraphs in Section 3.1, then present our adaptations that yield

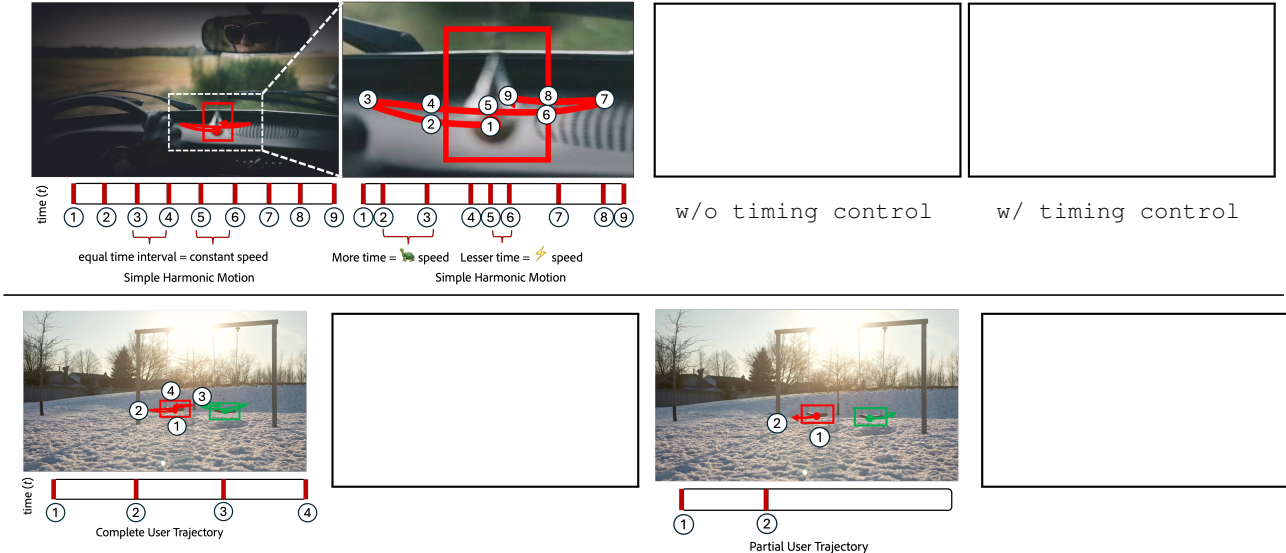


Figure 3. **Fine Grained Controls**. (top) **Timing controls**: Highlights a scenario where timing control is essential for realistic motion. User intends to simulate the bead oscillating in simple harmonic motion (SHM). Without timing control, i.e., equally space points (top-left) the bead has constant motion, not following SHM, thus looking unrealistic. With timing control, user can assign more time the extrema and lesser time at the minima of SHM, accurately simulating physically realistic motion. (bottom) **Full vs. Partial motion paths**: Demonstrate 2 scenarios of the same example, where the user can either provide the full motion path (bottom-left) or just the initial motion trajectory (bottom-right) and remaining is automatically generated with our model.

high-quality, controllable loops from a single input photo. We customize VDMs for cinemagraph generation by (i) enforcing seamless looping (Section 3.2), and (ii) enabling precise, user-guided control through motion conditioning on the provided bounding box sequences and point tracks (Section 3.3). Finally, in Section 3.4 we describe an easy and intuitive way for the user to provide motion control signals to our method.

### 3.1. Video Diffusion Models

Video diffusion models (VDMs) are large-scale generative models trained on millions of in-the-wild videos. Because our input is a single photograph, we focus on image-to-video (I2V) models. We build upon a pretrained DiT-based [42] I2V system: the input image is encoded by a 3D-VAE into spatiotemporal latents, the text prompt is encoded by a text encoder, and both are concatenated with noisy tokens and processed by a DiT transformer; a 3D-VAE decoder then transforms the latent to an RGB video. We use a variant trained with the flow-matching objective [34]. Let  $X^t$  denote the latent at time  $t \in [0, 1]$  and  $V^t$  are the target velocity along the training path. The model learns a velocity field  $v_\theta(\cdot, t)$  by minimizing the expected squared error:

$$\mathcal{L}_{\text{FM}}(\theta) = \min_{\theta} \|V^t - v_\theta(X^t, t)\|_2^2. \quad (1)$$

We leverage the rich motion priors learned by VDMs trained on massive, diverse video corpora as a starting point toward

single-image-to-cinemagraph generation.

**Cinemagraphs vs. videos.** Standard I2V VDMs are optimized to produce fully dynamic videos, whereas cinemagraphs contain mostly static scenes with motion confined to selected regions and required to loop seamlessly. Bridging this mismatch is non-trivial: one must preserve a static background, enforce the resulting videos to be looping smoothly, and provide precise, user-guided motion control for our task of controllable cinemagraph generation. The next sections describe how we transform the pretrained VDM to satisfy these cinemagraph-specific constraints.

### 3.2. Time Bridging with Temporal-Boundary Conditioning

At first glance, cinemagraphs differ from generic videos in that their motion must loop seamlessly and continuously. A seemingly straightforward way to adapt VDMs is to train them directly on cinemagraph datasets, but such data are scarce and often low quality. Instead, we exploit large-scale in-the-wild video data and train the VDM on the proxy task of time bridging to encourage the model to learn to interpret the temporal connection between two arbitrary point in time. We achieve this with the temporal-boundary conditioning strategy. Concretely, given a training clip  $\{I_t\}_{t=0}^T$ , we encode the boundary frames with the pretrained 3D-VAE encoder  $\mathcal{E}$  from the base DiT to obtain  $C_{I_0}, C_{I_T}$ . These tokens are concatenated to the diffusion tokens and provided to the transformer at all timesteps. At inference, a cinemagraph

becomes a special case by setting the boundary conditions equal to the input photo, i.e.,  $I_0 = I_T = I$ , which enforces a seamless loop. However, temporal-boundary conditioning alone is insufficient for controllable cinemagraphs. (i) Text prompts are often ambiguous and can yield incorrect or unexpected motion, especially in cases where users desire to have fine grained motion control; for example, in Figure 4 (bottom), the variant “Ours (temporal-boundary only)” hallucinates an additional person even though the user intent is to move only the hand and brush. (ii) In some cases, the model collapses to nearly static frames. We present additional failure cases in [website](#).

### 3.3. Motion Control

To address the limitations of only using temporal-boundary conditioning for cinemagraph generation and to capture user intent of fine-grained motion control, we further propose to augment the video generative model with object motion conditioning. To choose two forms of conditions for motion control with VDMs: (1) **Bounding Boxes**: We capture the object’s global motion using bounding boxes, which capture the spatial information of the object. For a video, given coordinates  $(x_1, y_1, x_2, y_2)$  for an object denoting the top-left and bottom-right corners, similar to MotionCanvas [58], we turn the coordinates into an RGB mask sequence  $C_{bbox}^{RGB} \in \mathbb{R}^{T' \times H' \times W' \times 3}$  with each object being color-coded with a unique color. This RGB mask is then encoded by the same 3D-VAE encoder  $\mathcal{E}$  to produce a spatiotemporal representation  $C_{bbox} = \mathcal{E}(C_{bbox}^{RGB})$ . (2) **Sparse Point Tracks**: Point tracks are useful for capturing local object motion. Additionally, a major advantage and our key insight for using point track conditioning for cinemagraphs is that the videos used for training VDMs often contain camera motion. To prevent undesirable motion in non-target regions during cinemagraph generation, we put static point tracks on those regions to keep them static when generating the cinemagraph. This immensely captures another key aspect of cinemagraphs, where certain regions of the image stay static, in an uncanny but aesthetic manner. Similar to the bounding boxes, we render  $N$  point trajectories using color-coded squares into an RGB sequence  $C_{traj}^{RGB} \in \mathbb{R}^{T' \times H' \times W' \times 3}$  and use  $\mathcal{E}$  to encode them, producing  $C_{traj} = \mathcal{E}(C_{traj}^{RGB})$ . The resulting tokens  $C_{motion} = (C_{bbox} \oplus C_{traj})$  are then added to the input noise tokens to the VDM. The final training objective is given by

$$\mathcal{L}_{FM}(\theta) = \min_{\theta} \|V^t - v_{\theta}(X^t, t | C_{I_0}, C_{I_T}, C_{motion}, C_{txt})\|_2^2, \quad (2)$$

where  $C_{txt}$  is the input prompt tokenized by the text encoder.

### 3.4. Capturing User Intent

Even though during training with motion control, we condition the VDMs for per-frame bounding box and trajectories,

during inference, it would be tedious for users to define per-frame motion conditions. Thus, we let the user specify a set of sparse bounding boxes (or trajectories) with timing control, and use spline interpolation to get the in-between dense bounding boxes or trajectories. We provide more details on inference and our demo user interface in [website](#).

### 3.5. Enabling fine-grained controls

**Full vs. Partial motion paths.** Our method provides users with full control over the motion pattern they want the selected moving elements to follow by specifying the full, detailed motion paths. However, there are scenarios where users simply want to control coarser motion information, such as the initial direction and speed of the movements. Our system also supports these use cases by enabling motion control with partial motion paths. For a video sequence of  $T$  frames, we allow users to specify the motion path of the target objects/regions for the first  $T' \in [1, T]$  frames. If the bounding boxes (or point tracks) are not provided for all  $T$  frames, the model is able to infer from the partial input to complete the sequence. This flexibility is enabled by randomly dropping varying amounts of the latter portion of the bounding box (or point tracks) sequences during training. For example, in Figure 3 (bottom), we see for the same input example, the user can provide either a full motion sequence (bottom-left) or just a partial sequence (bottom-right), and let the model interpret the remaining motion. Videos corresponding to the inputs are in [website](#).

**Refinement with region controls.** During inference, we fix the point trajectories to be static to disable camera motion (as shown in Figure 2 (Inference)). While in most cases the static trajectories also prevents motion of the background regions, there are special cases where small, textured regions may still have small local motion. This is likely a consequence of video priors where although many videos contain static content with respect to the *global* scene, there is often small *local* motion in these areas. To prevent motion in non-target regions, users may provide an optional mask which can be used to blend the original image with the generated output.

**Timing controls.** The motion paths of the dynamic regions can either be specified on a frame-by-frame basis or by interpolating between a set of anchor bounding boxes placed on the timeline (Section 3.4), which is much more easier for user than providing per-frame motion condition. The precise timing and speed of the motions can be controlled by adjusting the anchors on the timeline. One particular example scenario is described in Figure 3 (top), where the user wants to generate a cinemagraph of a metallic bead oscillating in a ‘*simple harmonic motion*’. In this example the user only inputs the bounding boxes at 1...9 discrete intervals, and remaining sequence is interpreted with spline interpolation. Without timing control the bead would move at an approximately uniform speed. However, to simulate

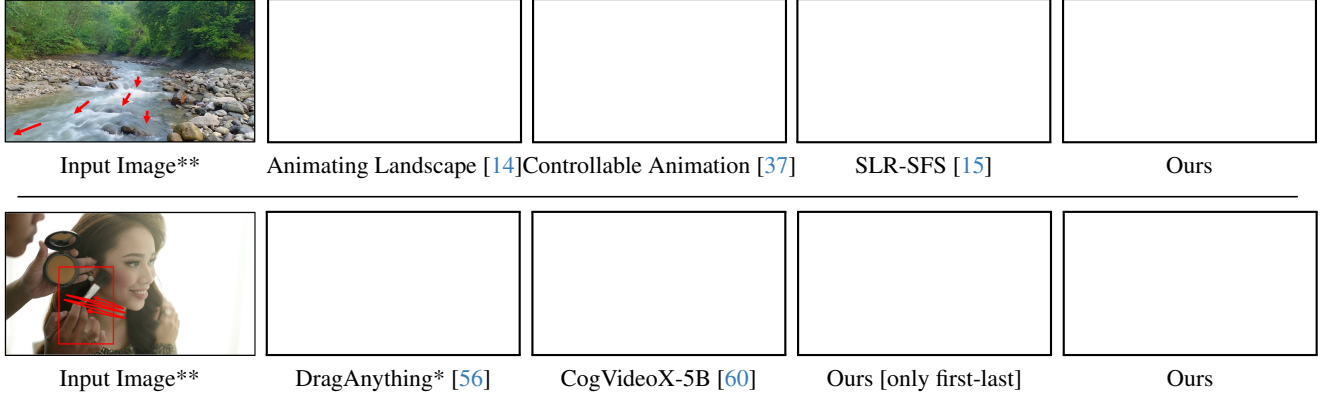


Figure 4. **Comparison with baselines.** Our full method (left) generates cinemagraphs with more realistic motion and accurately follows the input direction signal, both for the case of ‘*fluid-elements*’ cinemagraphs (top) and ‘*general-domain*’ cinemagraphs (bottom). (\*) Denotes we apply postprocessing from [14] to make the generated videos loop. (\*\*) Denotes arrows on inputs for motion representative purpose. *We encourage readers to view the videos in the figure with Acrobat Reader.*

Method	FVD	DT-FVD	KID	FID
Animating Landscape [14]	840.12	0.64	12.42	18.29
Text2Cinemagraph [38]	597.14	0.46	3.62	8.68
Wan2.2-5B* [51] (pretrained)	430.03	0.63	23.56	26.27
CogVideoX* [60]	782.68	2.14	57.81	38.11
Ours (Wan2.2-5B) [only first-last]	<b>306.36</b>	<b>0.31</b>	4.82	<b>7.14</b>
Ours (internal) [only first-last]	338.67	0.39	<b>3.46</b>	7.21

Table 1. **Quantitative Evaluation on ‘*fluid-elements*’ (Uncontrollable).** Comparison of our method with baselines using common video generation metrics. Bold numbers indicate the best performance per column. (\*) Denotes we apply postprocessing from [14] to make the generated videos loop.

realistic ‘*simple harmonic motion*’, user can assign longer dwell times near the extrema and shorter times near the center, thus inducing the characteristic slow–fast–slow ‘*simple harmonic motion*’ profile. Additional examples and videos illustrating the benefits of timing control are provided in [website](#).

## 4. Experiments

**Implementation Details.** We begin with a pretrained Image-to-Video (I2V) model and first finetune it for first–last frame-conditioned generation. We then extend training to incorporate bounding-box and trajectory control with  $\sim 8M$  videos. During this stage, we apply two conditioning dropout strategies: (i) randomly dropping between 0 and  $N$  bounding boxes or trajectory points across the sequence, and (ii) dropping all conditioning inputs after the first  $K$  frames to enable partial user-specified motion paths (Section 3.3). We train two variants of our method: one based on our internal model, finetuned to generate 3-second and 5-second videos at 1080p resolution, and one based on the Wan2.2-5B [51] model, finetuned for 3-second videos at 544p resolution. All

experiments are conducted on four A100 nodes. Additional architectural and training details are provided in [website](#).

**Evaluation.** Unlike prior works [14, 15, 22, 37, 38], which rely on optical-flow-based warping and are therefore limited to natural scenes with repeating textures (e.g., water, smoke), our method imposes no such restrictions. Nonetheless, because our approach is also applicable to these settings, we conduct two types of evaluations. (i) We compare against prior methods on cinemagraph generation for natural scenes such as rivers, lakes, and coastal water dynamics; we refer to this setting as ‘*Fluid-Elements Cinemagraphs*’. (ii) We additionally evaluate on a significantly more challenging regime involving arbitrary dynamic content, including humans, objects, and animals; we refer to this setting as ‘*General-Domain Cinemagraphs*’.

### 4.1. Fluid-Elements Cinemagraphs

**Evaluation Dataset and Metrics.** Following prior works [14, 15, 22, 37, 38], we evaluate our method and baselines on 162 nature-scene videos with fluid motion provided by [22], predominantly containing rivers, lakes, ocean etc. We evaluate them under two different settings: i) uncontrollable generation - only image as inputs, ii) controllable generation - with input image and direction guidance. Following [31] we evaluate the results on FVD [16, 50], DTFVD [13], FID [21, 28, 41] and KID [7]. The text-prompts corresponding to these examples are generated with GPT-5, and masks (of region to move in generated cinemagraphs) are generated with ODISE [59] following Text2Cinemagraph [38].

**Direction Guidance.** Under the controllable generation setting, we evaluate our method and baselines with 1 and 5 direction inputs (hints). to get these hints automatically, we following Controllable Animation [37], and perform K-Means clustering on the ground-truth optical flow in the

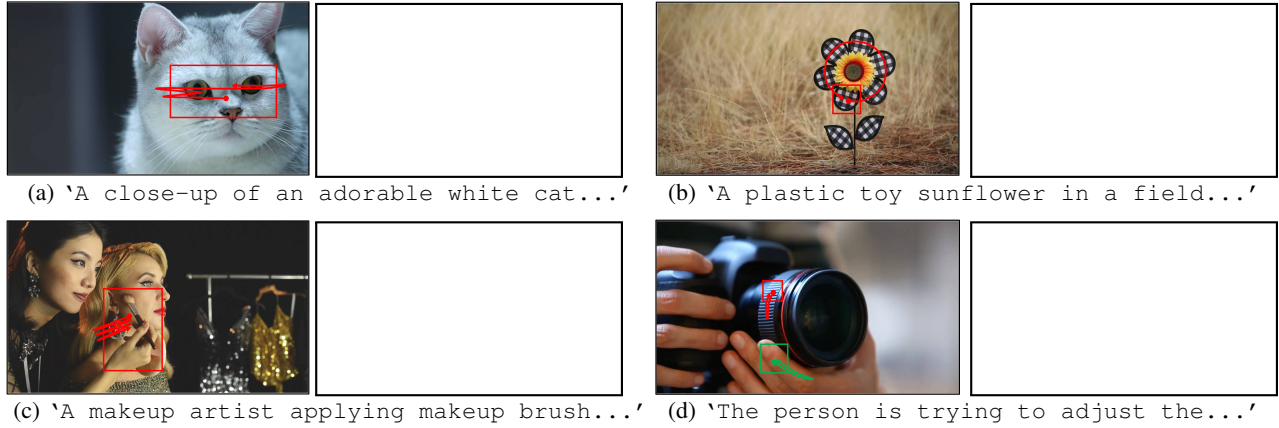


**Figure 5. Our Results.** Figure shows the robustness of our method to generate very diverse cinemagraphs with different motion patterns, like cat moving its head, or human applying makeup in translation motion. The toy flower petals rotating. (bottom-left) Our method can also simulate complex, realistic hand-object interaction with relatively simple input control signals. *We encourage readers to view the videos in the figure with Acrobat Reader.*

Method	FVD	DT-FVD	KID	FID
<b>[1 Hint Point]</b>				
Animating Landscape [14]	795.02	0.58	11.31	17.44
SLR-SFS [47]	402.34	0.33	6.87	9.28
Controllable Animation [37]	434.61	0.38	7.22	10.21
Ours (Wan2.2-5B)	<b>269.38</b>	<b>0.29</b>	4.62	<b>7.08</b>
Ours (internal)	286.34	0.3	<b>3.11</b>	7.24
<b>[5 Hint Points]</b>				
Animating Landscape [14]	773.71	0.56	11.97	17.61
SLR-SFS [47]	379.47	0.35	7.16	9.24
Controllable Animation [37]	414.78	0.38	7.92	10.06
Ours (Wan2.2-5B)	<b>256.73</b>	<b>0.29</b>	4.62	<b>7.09</b>
Ours (internal)	272.38	<b>0.29</b>	<b>3.33</b>	7.17

**Table 2. Quantitative Evaluation on 'fluid-elements' (Controllable).** Comparison of our method with baselines using common video generation metrics under single and multi-trajectory-point control settings. Bold numbers indicate the best performance per column. (\*) Denotes we apply postprocessing from [14] to make the generated videos loop.

dataset and identify 5 (or 1) clusters. We then propagate the optical flow value of these hints in the masked region of the image. These are treated as guidance optical flow maps for baselines. For our method we use this guidance optical flow map to generate per-frame point tracks. For evaluation purpose, we use point tracks on  $10 \times 10$  grid, similar to our training setting, thought our method is robust to different number of point tracks (examples in [website](#)).

**Baselines.** We evaluate our method under two broad categories. **(I) Uncontrollable Generation.** We compare against: (i) *Optical flow-based methods* — Animating Landscape [14] and Text2Cinemagraph [38]; and (ii) *Image-to-Video models* — CogVideoX-5B [60] and Wan2.2-5B [51]

(pretrained). We compare them against our model variant trained only with first–last frame conditioning for comparison. **(II) Controllable Generation.** We compare with controllable optical flow-based approaches, including Animating Landscape (control variant) [14], SLR-SFS [47], and Controllable Animation [37]. Following Controllable Animation [37], we evaluate these models using both one and five directional hints. Since Image-to-Video models do not inherently generate looping videos, we apply a post-processing procedure similar to that of Endo *et al.* [14] to produce seamless loops.

**Effectiveness on Uncontrollable Generation** From Table 1 shows that our method—using both Wan2.2-5B and our internal model—outperforms the baselines on all metrics — FVD, DT-FVD, KID, and FID. This improvement is largely due to leveraging VDMs, which yield more realistic motion than optical-flow-based warping baselines. Because Wan2.2-5B and CogVideoX produce non-looping videos, we apply post-processing to enforce looping; this can degrade frame quality, introducing blending artifacts, especially when the generated videos contain camera motion. We provide video results in [website](#) showing side-by-side comparisons, where our results exhibit noticeably more realistic motion. Additionally, our method with Wan2.2-5B backbone performs better than internal model which can be attributed to different learned priors.

**Effectiveness on Controllable Generation.** Similar to the scenario of Uncontrollable Generation, from Table 2, we find that for both 1-hint and 5-hints, our methods perform better than baselines in terms of all metrics. We see from Figure 4 (top) that optical flow-based baselines can generate unrealistic motion (Animating Landscape [14]), or have holes in the generated frames due to incorrect optical flow estimation or inability of the model to fill holes introduced

Method	Aesthetic Quality	Imaging Quality	Temporal Flickering	Motion Smoothness	Background Consistency	Subject Consistency
CogVideoX* [60]	0.5353	0.6419	0.9888	0.9904	0.9741	0.9787
Wan2.2-5B* [51] (pretrained)	0.5442	0.6018	0.9881	0.9922	0.9598	0.9605
DragAnything* [56]	0.4986	0.5535	0.9674	0.9789	0.9613	0.9474
Ours (Wan2.2-5B) [only first-last]	0.5897	0.6756	0.9950	0.9959	0.9746	0.9941
Ours (internal) [only first-last]	0.5872	0.6615	0.9899	0.9929	0.9685	0.9566
Ours (Wan2.2-5B)	<b>0.5998</b>	0.6762	0.9955	<b>0.9964</b>	0.9800	<b>0.9868</b>
Ours (internal)	0.5997	<b>0.6771</b>	<b>0.9965</b>	0.9959	<b>0.9849</b>	0.9858

Table 3. **Quantitative evaluation on ‘Rigid-Body Cinemagraphs’.** Comparison of our methods against baseline Image-to-Video and controllable generation models across multiple VBench [24] metrics. Bold numbers indicate the best performance per column. (\*) Denotes we apply postprocessing from [14] to make the generated videos loop.

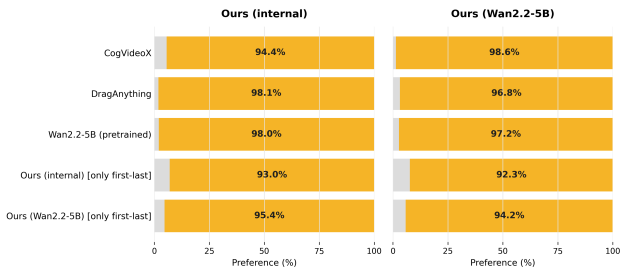


Figure 6. **User Study.** Figure shows user study of our method, with both internal model and Wan2.2-5B backbone. For both cases, users heavily favour cinemagraphs generated by our method compared to the baselines. Bright-yellow denotes percentage our methods is preferred over baselines.

by optical-flow warping (SLR-SFS [15]). In contrast, our method produces realistic water motion.

## 4.2. General-Domain Cinemagraphs

**Evaluation Dataset and Metrics.** For evaluating ‘General-Domain Cinemagraphs’, we manually curate a dataset consisting of 50 images, text prompts, along with corresponding bounding-box and trajectory annotations. The dataset spans a diverse range of scenes, including humans, animals, and inanimate objects. We evaluate our method and the baselines using multiple dimensions of VBench [24], specifically: *Aesthetic Quality*, *Imaging Quality*, *Temporal Flickering*, *Motion Smoothness*, *Background Consistency*, and *Subject Consistency*. For each sample, we conduct evaluations with three random seeds to account for the generation variability.

**Baselines.** We compare our method against three categories of baselines: (i) Image-to-Video models: CogVideoX-5B [60] and Wan2.2-5B [51] (pretrained); (ii) Trajectory-controlled Image-to-Video models: DragAnything [56]; and (iii) Our model variants trained with only first-last frame conditioning. For categories (i) and (iii), we use detailed text prompts derived from the corresponding motion conditions. Since models in categories (i) and (ii) do not inherently generate looping videos, we apply a post-processing procedure similar to that of Endo *et al.* [14] to produce seamless loops.

**User-Study.** We also conduct a user study to assess the quality of generated cinemagraphs. We ask the Amazon MTurk participants to choose which animation they prefer, based on following the bounding box and trajectory control. We perform paired tests, where the users are asked to compare two videos, one generated by our method and the other by one of the baselines. The study was conducted with 50 annotators, where each paired comparison was annotated by three annotators. More details about the User Study are in [website](#).

**Effectiveness on ‘General-Domain Cinemagraphs’.** From Table 3, we see that our method, with both Wan2.2-5B and internal model, outperforms all baselines and our method with only first- and last-frame conditions for controllable cinemagraph generation. Specifically, from Figure 4 (bottom), DragAnything and CogVideoX have blending artifacts due to post-processing to make them loop. Our method, with only first- and last-frame conditions, unexpectedly introduces a human, even though it was not expressed in the input user intent. Our method generates the cinemagraph, precisely capturing the user input. Figure 6 shows that users extensively prefer cinemagraphs generated by our method over baselines by a huge margin. Our method can generate cinemagraphs for diverse scenes, like animals (cat), humans, objects, with different motion patterns like translation (cat head and human applying makeup), rotation (flower), and can capture object interaction accurately (Figure 6 (bottom-right)).

## 5. Conclusion and Limitations

This paper presented DreamLoop, a controllable cinemagraph generation technology. It empowers a user to animate any image content with intuitive control of object motion when creating cinemagraphs from a single photo. DreamLoop is built upon a pre-trained image-to-video model and fine-tuned with widely available regular videos without cinemagraphs that are difficult to obtain at scale. The two key enabling innovations of our method are temporal bridging that enables the model to generate loop animation and motion conditioning that allows a user to animate desirable content while keeping the rest of image content static. As

demonstrated in the experiments, this technology significantly simplifies high-quality cinemagraph production.

**Limitations.** Even though our method can generate high-quality cinemagraphs capturing user motion guidance with precise timing control, there are still some failure cases: (1) Because our method is built on top of VDMs, occasionally generated cinemagraphs can have morphing artifacts or implausible motion common to VDMs. (2) Even though we provide static point tracks for regions with no user-guided motion, certain generations can still have in-place small motion. Though they can be corrected with blending using masks. (3) In scenarios when the user-provided direction annotations may be conflicting with each other or physically implausible, the model might ignore one or more motion conditions in the generated cinemagraphs, which may be unsatisfactory for the user. We provide more such cases and video examples in [website](#).

## References

- [1] Aseem Agarwala, Ke Colin Zheng, Chris Pal, Maneesh Agrawala, Michael Cohen, Brian Curless, David Salesin, and Richard Szeliski. Panoramic video textures. In *ACM SIGGRAPH 2005 Papers*, pages 821–827. 2005. 2
- [2] Sherwin Bahmani, Ivan Skorokhodov, Guocheng Qian, Aliaksandr Siarohin, Willi Menapace, Andrea Tagliasacchi, David B. Lindell, and Sergey Tulyakov. Ac3d: Analyzing and improving 3d camera control in video diffusion transformers. *arXiv preprint arXiv:2411.18673*, 2024. 3
- [3] Jiamin Bai, Aseem Agarwala, Maneesh Agrawala, and Ravi Ramamoorthi. Selectively de-animating video. *ACM Trans. Graph.*, 31(4):66–1, 2012. 2
- [4] Jiamin Bai, Aseem Agarwala, Maneesh Agrawala, and Ravi Ramamoorthi. Automatic cinemagraph portraits. In *Computer Graphics Forum*, pages 17–25. Wiley Online Library, 2013. 2
- [5] Omer Bar-Tal, Hila Chefer, Omer Tov, Charles Herrmann, Roni Paiss, Shiran Zada, Ariel Ephrat, Junhwa Hur, Guanghui Liu, Amit Raj, et al. Lumiere: A space-time diffusion model for video generation. In *SIGGRAPH Asia 2024 Conference Papers*, 2024. 3
- [6] Hugo Bertiche, Niloy J Mitra, Kuldeep Kulkarni, Chun-Hao Paul Huang, Tuanfeng Y Wang, Meysam Madadi, Sergio Escalera, and Duygu Ceylan. Blowing in the wind: Cyclenet for human cinemagraphs from still images. *arXiv preprint arXiv:2303.08639*, 2023. 2
- [7] Mikołaj Bińkowski, Daniela J Sutherland, Michael Arbel, and Arthur Gretton. Demystifying mmd gans. In *International Conference on Learning Representations (ICLR)*, 2018. 6
- [8] Andreas Blattmann, Tim Dockhorn, Sumith Kulal, Daniel Mendelevitch, Maciej Kilian, Dominik Lorenz, Yam Levi, Zion English, Vikram Voleti, Adam Letts, et al. Stable video diffusion: Scaling latent video diffusion models to large datasets. *arXiv preprint arXiv:2311.15127*, 2023. 3
- [9] Tim Brooks, Bill Peebles, Connor Holmes, Will DePue, Yufei Guo, Li Jing, David Schnurr, Joe Taylor, Troy Luhman, Eric Luhman, Clarence Ng, Ricky Wang, and Aditya Ramesh. Video generation models as world simulators. 2024.
- [10] Haoxin Chen, Menghan Xia, Yingqing He, Yong Zhang, Xiaodong Cun, Shaoshu Yang, Jinbo Xing, Yaofang Liu, Qifeng Chen, Xintao Wang, et al. VideoCrafter1: Open diffusion models for high-quality video generation. *arXiv preprint arXiv:2310.19512*, 2023. 3
- [11] Ho Kei Cheng, Seoung Wug Oh, Brian Price, Alexander Schwing, and Joon-Young Lee. Tracking anything with decoupled video segmentation. In *ICCV*, 2023. 12
- [12] Yung-Yu Chuang, Dan B Goldman, Ke Colin Zheng, Brian Curless, David H Salesin, and Richard Szeliski. Animating pictures with stochastic motion textures. In *ACM SIGGRAPH 2005 Papers*, pages 853–860. 2005. 2
- [13] Michael Dorkenwald, Timo Milbich, Andreas Blattmann, Robin Rombach, Konstantinos G Derpanis, and Björn Ommer. Stochastic image-to-video synthesis using cinns. In *Proceedings of the IEEE/CVF Conference on Computer Vision and Pattern Recognition*, pages 3742–3753, 2021. 6
- [14] Yuki Endo, Yoshihiro Kanamori, and Shigeru Kuriyama. Animating landscape: self-supervised learning of decoupled motion and appearance for single-image video synthesis. *arXiv preprint arXiv:1910.07192*, 2019. 2, 6, 7, 8
- [15] Siming Fan, Jingtan Piao, Chen Qian, Kwan-Yee Lin, and Hongsheng Li. Simulating fluids in real-world still images. *arXiv preprint arXiv:2204.11335*, 2022. 2, 3, 6, 8
- [16] Songwei Ge, Aniruddha Mahapatra, Gaurav Parmar, Jun-Yan Zhu, and Jia-Bin Huang. On the content bias in fréchet video distance. In *Proceedings of the IEEE/CVF Conference on Computer Vision and Pattern Recognition (CVPR)*, 2024. 6
- [17] Yoav HaCohen, Nisan Chiprut, Benny Brazowski, Daniel Shalem, Dudu Moshe, Eitan Richardson, Eran Levin, Guy Shiran, Nir Zabari, Ori Gordon, et al. Ltx-video: Realtime video latent diffusion. *arXiv preprint arXiv:2501.00103*, 2024. 3
- [18] Tavi Halperin, Hanit Hakim, Orestis Vantzos, Gershon Hochman, Netai Benaim, Lior Sassy, Michael Kupchik, Ofir Bibi, and Ohad Fried. Endless loops: Detecting and animating periodic patterns in still images. *ACM Trans. Graph.*, 40(4), 2021. 2, 3
- [19] Hao He, Yinghao Xu, Yuwei Guo, Gordon Wetzstein, Bo Dai, Hongsheng Li, and Ceyuan Yang. Cameractrl: Enabling camera control for text-to-video generation. *arXiv preprint arXiv:2404.02101*, 2024. 3
- [20] Mingming He, Jing Liao, Pedro V Sander, and Hugues Hoppe. Gigapixel panorama video loops. *ACM Transactions on Graphics (TOG)*, 37(1):1–15, 2017. 2
- [21] Martin Heusel, Hubert Ramsauer, Thomas Unterthiner, Bernhard Nessler, and Sepp Hochreiter. Gans trained by a two time-scale update rule converge to a local nash equilibrium. In *Conference on Neural Information Processing Systems (NeurIPS)*, 2017. 6
- [22] Aleksander Holynski, Brian L Curless, Steven M Seitz, and Richard Szeliski. Animating pictures with eulerian motion fields. In *Proceedings of the IEEE/CVF Conference on Computer Vision and Pattern Recognition*, pages 5810–5819, 2021. 2, 3, 6
- [23] Hsin-Ping Huang, Yu-Chuan Su, Deqing Sun, Lu Jiang, Xuhui Jia, Yukun Zhu, and Ming-Hsuan Yang. Fine-grained

- controllable video generation via object appearance and context. In *WACV*, 2025. 3
- [24] Ziqi Huang, Yinan He, Jiashuo Yu, Fan Zhang, Chenyang Si, Yuming Jiang, Yuanhan Zhang, Tianxing Wu, Qingyang Jin, Nattapol Chanpaisit, et al. Vbench: Comprehensive benchmark suite for video generative models. In *Proceedings of the IEEE/CVF Conference on Computer Vision and Pattern Recognition*, pages 21807–21818, 2024. 8
- [25] Neel Joshi, Sisil Mehta, Steven Drucker, Eric Stollnitz, Hugues Hoppe, Matt Uyttendaele, and Michael Cohen. Cliplets: juxtaposing still and dynamic imagery. In *Proceedings of the 25th annual ACM symposium on User interface software and technology*, pages 251–260, 2012. 2
- [26] Weijie Kong, Qi Tian, Zijian Zhang, Rox Min, Zuozhuo Dai, Jin Zhou, Jiangfeng Xiong, Xin Li, Bo Wu, Jianwei Zhang, Kathrina Wu, Qin Lin, Aladdin Wang, Andong Wang, Changlin Li, Duojun Huang, Fang Yang, Hao Tan, Hongmei Wang, Jacob Song, Jiawang Bai, Jianbing Wu, Jinbao Xue, Joey Wang, Junkun Yuan, Kai Wang, Mengyang Liu, Pengyu Li, Shuai Li, Weiyang Wang, Wenqing Yu, Xinchi Deng, Yang Li, Yanxin Long, Yi Chen, Yutao Cui, Yuanbo Peng, Zhen-tao Yu, Zhiyu He, Zhiyong Xu, Zixiang Zhou, Zunnan Xu, Yangyu Tao, Qinglin Lu, Songtao Liu, Dax Zhou, Hongfa Wang, Yong Yang, Di Wang, Yuhong Liu, Jie Jiang, and Caesar Zhong. Hunyuvideo: A systematic framework for large video generative models, 2024. 2
- [27] Vivek Kwatra, Arno Schödl, Irfan Essa, Greg Turk, and Aaron Bobick. Graphcut textures: Image and video synthesis using graph cuts. *AcM transactions on graphics (tog)*, 22(3):277–286, 2003. 2
- [28] Tuomas Kynkänniemi, Tero Karras, Samuli Laine, Jaakko Lehtinen, and Timo Aila. Improved precision and recall metric for assessing generative models. In *Conference on Neural Information Processing Systems (NeurIPS)*, 2019. 6
- [29] Pengxiang Li, Zhili Liu, Kai Chen, Lanqing Hong, Yunzhi Zhuge, Dit-Yan Yeung, Huchuan Lu, and Xu Jia. Trackdiffusion: Multi-object tracking data generation via diffusion models. *arXiv preprint arXiv:2312.00651*, 2023. 3
- [30] Xingyi Li, Zhiguo Cao, Huiqiang Sun, Jianming Zhang, Ke Xian, and Guosheng Lin. 3d cinematography from a single image. *arXiv preprint arXiv:2303.05724*, 2023. 2
- [31] Zhengqi Li, Richard Tucker, Noah Snavely, and Aleksander Holynski. Generative image dynamics. In *Proceedings of the IEEE/CVF Conference on Computer Vision and Pattern Recognition (CVPR)*, 2024. 6
- [32] Jing Liao, Mark Finch, and Hugues Hoppe. Fast computation of seamless video loops. *ACM Transactions on Graphics (TOG)*, 34(6):1–10, 2015. 2
- [33] Zicheng Liao, Neel Joshi, and Hugues Hoppe. Automated video looping with progressive dynamism. *ACM Transactions on Graphics (TOG)*, 32(4):1–10, 2013. 2
- [34] Yaron Lipman, Ricky TQ Chen, Heli Ben-Hamu, Maximilian Nickel, and Matt Le. Flow matching for generative modeling. *arXiv preprint arXiv:2210.02747*, 2022. 4
- [35] Elizaveta Logacheva, Roman Suvorov, Oleg Khomenko, Anton Mashikhin, and Victor Lempitsky. Deeplandscape: Adversarial modeling of landscape videos. In *Computer Vision–ECCV 2020: 16th European Conference, Glasgow, UK, August 23–28, 2020, Proceedings, Part XXIII 16*, pages 256–272, 2020. 2
- [36] Wan-Duo Kurt Ma, J. P. Lewis, and W. Bastiaan Kleijn. Trailblazer: Trajectory control for diffusion-based video generation, 2023. 3
- [37] Aniruddha Mahapatra and Kuldeep Kulkarni. Controllable animation of fluid elements in still images. In *Proceedings of the IEEE/CVF Conference on Computer Vision and Pattern Recognition*, pages 3667–3676, 2022. 2, 3, 6, 7
- [38] Aniruddha Mahapatra, Aliaksandr Siarohin, Hsin-Ying Lee, Sergey Tulyakov, and Jun-Yan Zhu. Text-guided synthesis of eulerian cinemagraphs. *ACM Transactions on Graphics (TOG)*, 42(6):1–13, 2023. 2, 3, 6, 7
- [39] Chong Mou, Mingdeng Cao, Xintao Wang, Zhaoyang Zhang, Ying Shan, and Jian Zhang. Revideo: Remake a video with motion and content control. *arXiv preprint arXiv:2405.13865*, 2024. 3
- [40] Muyao Niu, Xiaodong Cun, Xintao Wang, Yong Zhang, Ying Shan, and Yinqiang Zheng. MOFA-video: Controllable image animation via generative motion field adaptions in frozen image-to-video diffusion model. In *European Conference on Computer Vision (ECCV)*, 2024. 3
- [41] Gaurav Parmar, Richard Zhang, and Jun-Yan Zhu. On aliased resizing and surprising subtleties in gan evaluation. In *Proceedings of the IEEE/CVF conference on computer vision and pattern recognition*, pages 11410–11420, 2022. 6
- [42] William Peebles and Saining Xie. Scalable diffusion models with transformers. In *Proceedings of the IEEE/CVF international conference on computer vision*, pages 4195–4205, 2023. 4
- [43] Adam Polyak, Amit Zohar, Andrew Brown, Andros Tjandra, Animesh Sinha, Ann Lee, Apoorv Vyas, Bowen Shi, Chih-Yao Ma, Ching-Yao Chuang, et al. Movie Gen: A cast of media foundation models. *arXiv preprint arXiv:2410.13720*, 2024. 3
- [44] Lu Qi, Jason Kuen, Tiancheng Shen, Jiuxiang Gu, Weidong Guo, Jiaya Jia, Zhe Lin, and Ming-Hsuan Yang. High-quality entity segmentation. In *International Conference on Computer Vision (ICCV)*, 2023. 12
- [45] Arno Schödl, Richard Szeliski, David H Salesin, and Irfan Essa. Video textures. In *Proceedings of the 27th annual conference on Computer graphics and interactive techniques*, pages 489–498, 2000. 2
- [46] Laura Sevilla-Lara, Jonas Wulff, Kalyan Sunkavalli, and Eli Shechtman. Smooth loops from unconstrained video. In *Computer Graphics Forum*, pages 99–107. Wiley Online Library, 2015. 2
- [47] Edgar Simo-Serra, Satoshi Iizuka, Kazuma Sasaki, and Hiroshi Ishikawa. Learning to simplify: fully convolutional networks for rough sketch cleanup. *ACM Transactions on Graphics (TOG)*, 35(4):1–11, 2016. 2, 7
- [48] Zachary Teed and Jia Deng. Raft: Recurrent all-pairs field transforms for optical flow. In *Computer Vision–ECCV 2020: 16th European Conference, Glasgow, UK, August 23–28, 2020, Proceedings, Part II 16*, pages 402–419. Springer, 2020. 12

- [49] James Tompkin, Fabrizio Pece, Kartic Subr, and Jan Kautz. Towards moment imagery: Automatic cinemagraphs. In *2011 Conference for Visual Media Production*, pages 87–93. IEEE, 2011. 2
- [50] Thomas Unterthiner, Sjoerd Van Steenkiste, Karol Kurach, Raphael Marinier, Marcin Michalski, and Sylvain Gelly. Towards accurate generative models of video: A new metric & challenges. *arXiv preprint arXiv:1812.01717*, 2018. 6
- [51] Team Wan, Ang Wang, Baole Ai, Bin Wen, Chaojie Mao, Chen-Wei Xie, Di Chen, Feiwu Yu, Haiming Zhao, Jianxiao Yang, Jianyuan Zeng, Jiayu Wang, Jingfeng Zhang, Jingen Zhou, Jinkai Wang, Jixuan Chen, Kai Zhu, Kang Zhao, Keyu Yan, Lianghua Huang, Mengyang Feng, Ningyi Zhang, Pandeng Li, Pingyu Wu, Ruihang Chu, Ruili Feng, Shiwei Zhang, Siyang Sun, Tao Fang, Tianxing Wang, Tianyi Gui, Tingyu Weng, Tong Shen, Wei Lin, Wei Wang, Wei Wang, Wenmeng Zhou, Wente Wang, Wenting Shen, Wenyuan Yu, Xianzhong Shi, Xiaoming Huang, Xin Xu, Yan Kou, Yangyu Lv, Yifei Li, Yijing Liu, Yiming Wang, Yingya Zhang, Yitong Huang, Yong Li, You Wu, Yu Liu, Yulin Pan, Yun Zheng, Yuntao Hong, Yupeng Shi, Yutong Feng, Zeyinzi Jiang, Zhen Han, Zhi-Fan Wu, and Ziyu Liu. Wan: Open and advanced large-scale video generative models. *arXiv preprint arXiv:2503.20314*, 2025. 2, 6, 7, 8, 12
- [52] Jiawei Wang, Yuchen Zhang, Jiaxin Zou, Yan Zeng, Guoqiang Wei, Liping Yuan, and Hang Li. Boximator: Generating rich and controllable motions for video synthesis. In *International Conference on Machine Learning (ICML)*, 2024. 3
- [53] Xi Wang, Robin Courant, Marc Christie, and Vicky Kalogeiton. Akira: Augmentation kit on rays for optical video generation. *arXiv preprint arXiv:2412.14158*, 2024. 3
- [54] Zhouxia Wang, Ziyang Yuan, Xintao Wang, Yaowei Li, Tianshui Chen, Menghan Xia, Ping Luo, and Ying Shan. Motionctrl: A unified and flexible motion controller for video generation. In *ACM SIGGRAPH 2024 Conference Papers*, pages 1–11, 2024. 3
- [55] Jianzong Wu, Xiangtai Li, Yanhong Zeng, Jiangning Zhang, Qianyu Zhou, Yining Li, Yunhai Tong, and Kai Chen. Motionbooth: Motion-aware customized text-to-video generation. *NeurIPS*, 2024. 3
- [56] Weijia Wu, Zhuang Li, Yuchao Gu, Rui Zhao, Yefei He, David Junhao Zhang, Mike Zheng Shou, Yan Li, Tingting Gao, and Di Zhang. Draganything: Motion control for anything using entity representation, 2024. 3, 6, 8
- [57] Jinbo Xing, Menghan Xia, Yong Zhang, Haoxin Chen, Wangbo Yu, Hanyuan Liu, Gongye Liu, Xintao Wang, Ying Shan, and Tien-Tsin Wong. DynamiCrafter: Animating open-domain images with video diffusion priors. In *European Conference on Computer Vision (ECCV)*, 2024. 3
- [58] Jinbo Xing, Long Mai, Cusuh Ham, Jiahui Huang, Anirudha Mahapatra, Chi-Wing Fu, Tien-Tsin Wong, and Feng Liu. Motioncanvas: Cinematic shot design with controllable image-to-video generation. In *Proceedings of the Special Interest Group on Computer Graphics and Interactive Techniques Conference Conference Papers*, pages 1–11, 2025. 3, 5
- [59] Jiarui Xu, Sifei Liu, Arash Vahdat, Wonmin Byeon, Xiaolong Wang, and Shalini De Mello. Open-vocabulary panoptic segmentation with text-to-image diffusion models. *arXiv preprint arXiv:2303.04803*, 2023. 6
- [60] Zhuoyi Yang, Jiayan Teng, Wendi Zheng, Ming Ding, Shiyu Huang, Jiazheng Xu, Yuanming Yang, Wenyi Hong, Xiaohan Zhang, Guanyu Feng, et al. Cogvideox: Text-to-video diffusion models with an expert transformer. *arXiv preprint arXiv:2408.06072*, 2024. 2, 3, 6, 7, 8
- [61] Wangbo Yu, Jinbo Xing, Li Yuan, Wenbo Hu, Xiaoyu Li, Zhipeng Huang, Xiangjun Gao, Tien-Tsin Wong, Ying Shan, and Yonghong Tian. Viewcrafter: Taming video diffusion models for high-fidelity novel view synthesis. *arXiv preprint arXiv:2409.02048*, 2024. 3

## A. Training Details.

**Training Dataset.** Our training dataset consists of  $\sim 8$  Million videos annotated with bounding boxes and sparse point tracks, on a  $10 \times 10$  grid. The bounding boxes were extracted from ground-truth video using DEVA [11] and Qi et al. [44]. Point tracks were computed using optical flow. We first compute both forward and backward optical flows for the video using RAFT [48], and only keep those point trajectories for which cyclic consistency holds with forward and backward flows. Sparse point tracks are sampled on a uniform  $10 \times 10$  grid.

**Control Condition Details.** We condition the model with both bounding boxes and trajectories: (1) Bounding Box: From all the bounding box sequences for a sample video, we select up to three bounding boxes per iteration. The selection is random with multinomial sampling based on the area of the bounding box (with larger having more probability) for 80% and completely random for 20%. The selected boxes are rendered to frames of the same shape as the training video, with a black background. We use one of the RGB channels to encode the bounding boxes; hence, we train with a maximum of 3 bounding boxes. Note: that we can train with more bounding boxes with a different color scheme. This conditioning mechanism is not the primary focus of the work. (2) Sparse Point Tracks: Similar to bounding boxes, we render the point tracks on frames of the same shape as the training video with a black background as a square of 10 pixels. The color for each point track is based on its  $(x, y)$  coordinate. During training, we randomly drop 1...N point tracks. Both bounding boxes and point trajectories, once rendered to frames, are passed through the pretrained 3DVAE and added to the noisy latent after patchification. For both conditioning mechanisms, during training, with 50% probability, we randomly both bounding box and point track conditioning after K frames, where K is sampled uniformly between  $[0, N]$ , where N is the total number of frames. We do this to simulate the scenario where the user inputs a partial motion path.

**Training Procedure.** We finetune our models on 4 A100 nodes, consisting of 8 GPUs each, starting from a base Image-to-video model. For Wan2.2-5B [51], we finetune the model at 544p resolution videos of length 3s (73 frames), starting from the TI2V model. We first finetune the model with first-last-frame conditioning for 10K iterations. The last frame is concatenated in the token dimension as clean latent (similar to what Wan2.2-5B does for Image-to-Video training with the first frame). We further add bounding box and point track conditioning and fine-tune the model for an additional 10K iterations. We use the same learning rate, optimizer, and noise scheduler used in the original model training. For our method’s variant with our internal model, we follow a similar procedure, except that the base model is finetuned for 1080p videos of duration 3s and 5s (73 and

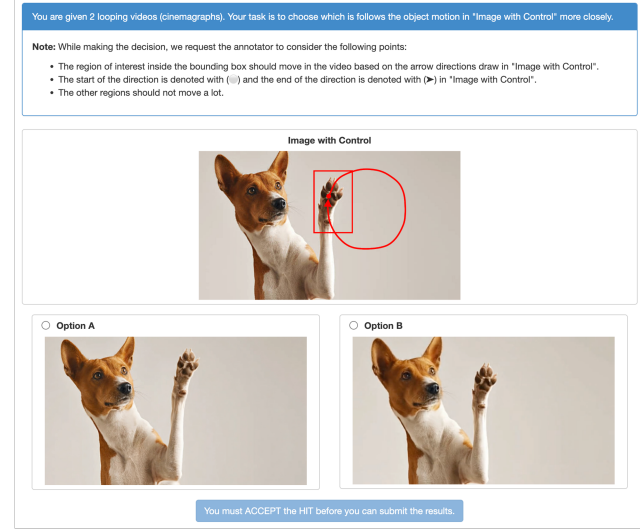


Figure 7. **User Study.** The figure shows the user study setup of our method on Amazon Mechanical Turk. Annotators are shown these instructions and the input image with reference motion path and asked which looping video they find to be better, following the representative motion path.

121 frames, respectively).

## B. User Study.

We conduct a user study on Amazon Mechanical Turk (AMT) using a set of 50 controllable cinemagraph videos. The study involves 50 unique annotators, and each video pair is evaluated by three independent workers. Figure 7 illustrates the AMT interface used for the pairwise comparisons. Given an input image and its corresponding motion-control specification overlaid on the image, annotators are asked to select ‘which of the two generated videos better follows the prescribed motion control’. To avoid confusion arising from unfamiliar terminology, we replace the word cinemagraph with the more widely understood term looping video in all user-facing instructions. We conduct two separate user studies: (1) comparing our internal model against all baselines, and (2) comparing Wan2.2-5B against the same set of baselines.